Available online at www.sciencedirect.com
ScienceDirect
Ceramics International 38S (2012) S163–S167
CERAMICS INTERNATIONAL
www.elsevier.com/locate/ceramint

Microwave dielectric properties of $(Zn_{1/3}B_{2/3})_{0.5}(Ti_{0.8}M_{0.2})_{0.5}O_2$ (B = Nb^{5+}, Ta^{5+}, M = Sn^{4+}, Ge^{4+}) ceramics

Eung Soo Kim *, Seock No Seo

Department of Materials Engineering, Kyonggi University, Suwon 443-760, Republic of Korea

Abstract

Dielectric properties of $(Zn_{1/3}Nb_{(2-x)/3}Ta_{x/3})_{0.5}(Ti_{0.8}Sn_{0.1}Ge_{0.1})_{0.5}O_2$ ($x = 0, 1, 2$) and/or $(Zn_{1/3}Nb_{1/3}Ta_{1/3})_{0.5}(Ti_{0.8}Sn_{0.2(1-y)}Ge_{0.2y})_{0.5}O_2$ ($y = 0, 0.5, 1$) were investigated at the microwave frequencies. For the compositions with single phase of rutile structure, the dielectric constant (K) of specimens was not only dependent on the dielectric polarizabilities, but also on the bond length ratio of apical bond (d_{apical}) to equatorial bond ($d_{equatorial}$) of oxygen octahedron in the unit cell. Temperature coefficients of the resonant frequencies (TCF) of the specimens with B = Nb^{5+} and/or M = Sn^{4+} was larger than those with B = Ta^{5+} and/or M = Ge^{4+}. These results could be attributed to the changes of the degree of oxygen octahedral distortion. Quality factors (Qf) of the specimens with B = Ta^{5+} and/or M = Sn^{4+} were larger than those with B = Nb^{5+} and/or M = Ge^{4+}.

Keywords: C. Dielectric properties; Ceramics; Crystal structure; Bond length ratio

1. Introduction

Microwave dielectric properties of ceramics are affected by the crystal structure and interactions between cation and anion of the compounds. It is necessary to understand the basic relationships for the simple structure, such as the rutile structure which has only two oxygen octahedra in the unit cell of crystal structure, to search the new dielectric materials and to control the microwave dielectric properties of ceramics effectively.

For the tetragonal rutile structure ($P4_2/mnm$, No.136, $Z = 2$), there are only two oxygen octahedra in the unit-cell, and these octahedra form chains by sharing corners and edges at each cation–oxygen bond. The oxygen octahedron of rutile structure consisted of four equatorial cation–oxygen bonds ($d_{equatorial}$) and two apical cation–oxygen bonds (d_{apical}), is slightly distorted if the apical cation–oxygen bonds are longer slightly than the other equatorial bond [1].

The substitution of Ti^{4+} ions of TiO_2 by other ions would affect the crystal structures and the microwave dielectric properties of the specimens. Dielectric constant (K) at microwave frequencies was found to be affected by the rattling of center ions of oxygen octahedron, and the temperature coefficient of resonant frequency (TCF) was closely related with the temperature coefficient of dielectric constant (TCK), which depended on the distortion of oxygen octahedron [2]. Also, the rattling effect of oxygen octahedron center ions and the octahedral distortion were largely dependent on the bond strength and bond length of the composing ions.

To clarify the effect of structural characteristics on the microwave dielectric properties of compound with rutile structure, it is interesting to study the substitutional effects of composing ions with same ionic size ($Nb^{5+} = Ta^{5+} = 0.64$ Å) [3] and/or different ionic sizes ($Ge^{4+} = 0.53$ Å, $Ti^{4+} = 0.605$ Å, $Sn^{4+} = 0.69$ Å) [3] on the microwave dielectric properties of the $(Zn_{1/3}B_{2/3})_{0.5}(Ti_{0.8}M_{0.2})_{0.5}O_2$ (B = Nb^{5+}, Ta^{5+}, M = Sn^{4+}, Ge^{4+}) ceramics.

Therefore, this study was focused on the substitutional effects of Ta^{5+} for Nb^{5+} of $(Zn_{1/3}B_{2/3})_{0.5}(Ti_{0.8}Sn_{0.1}Ge_{0.1})_{0.5}O_2$ (B = Nb^{5+}, Ta^{5+}) and Ge^{4+} for Sn^{4+} of $(Zn_{1/3}Nb_{1/3}Ta_{1/3})_{0.5}(Ti_{0.8}M_{0.2})_{0.5}O_2$ (M = Sn^{4+}, Ge^{4+}) on the microwave dielectric properties of the compound with rutile structures.

2. Experimental procedures

Raw materials of oxide powders with high purity (99.9%) were weighed according to the compositions of $(Zn_{1/3}Nb_{(2-x)/3}Ta_{x/3})O_2$ ($x = 0, 1, 2$) and $(Ti_{0.8}Sn_{0.2(1-y)}Ge_{0.2y})O_2$ ($y = 0, 0.5,$

---

* Corresponding author. Tel.: +82 31 249 9764; fax: +82 31 244 6300.
E-mail address: eskim@kyonggi.ac.kr (E.S. Kim).

0272-8842/$36.00 © 2011 Elsevier Ltd and Techna Group S.r.l. All rights reserved.
doi:10.1016/j.ceramint.2011.04.072

1), and milled with ZrO_2 balls for 24 h in distilled water, and then calcined at 1200 °C and 1150 °C for 3 h, respectively. These calcined powders were mixed according to the formula of $(Zn_{1/3}Nb_{(2-x)/3}Ta_{x/3})_{0.5}(Ti_{0.8}Sn_{0.1}Ge_{0.1})_{0.5}O_2$ ($x = 0, 1, 2$) and/or $(Zn_{1/3}Nb_{1/3}Ta_{1/3})_{0.5}(Ti_{0.8}Sn_{0.2(1-y)}Ge_{0.2y})_{0.5}O_2$ ($y = 0, 0.5, 1$) and re-calcined at 1200 °C for 3 h. The calcined powders were milled again for 24 h and then dried. The dried powders were pressed at 147 MPa isostatically. These pellets were sintered at 1250 °C for 3 h in air. The heating rate was 5 °C/min and the cooling rate was 1 °C/min down to 900 °C, and then furnace cooled to room temperature.

Powder X-ray diffraction (XRD) analyses (D/Max-3C, Rigaku, Japan) were used to determine the phase identification. The lattice parameters, unit-cell volumes and atomic positions were obtained from Rietveld refinements of XRD patterns. The Rietveld refinements were performed using the Full-Prof program [4]. The initial structure model for rutile compounds was taken from the work by Abrahams et al. [5]. The microstructure of the specimens was observed using a scanning electron microscope (SEM, JSM-6500F, JEOL, Japan). The microwave dielectric properties were measured by Hakki and Coleman's method [6] with the TE_{011} mode at 10–11 GHz. The *TCF* was measured by the cavity method [7] in the temperature range from 25 °C to 80 °C.

3. Results and discussion

The complete solid solutions of $(Zn_{1/3}Nb_{(2-x)/3}Ta_{x/3})_{0.5}(Ti_{0.8}Sn_{0.2(1-y)}Ge_{0.2y})_{0.5}O_2$ ($x = 0, 1, 2, y = 0, 0.5, 1$, $(ZNT)(TSG)O_2$) with tetragonal rutile structure ($P4_2/mnm$) were obtained through the entire range of compositions, as shown in Fig. 1. Crystal structure data (lattice parameters and unit cell volume) obtained from the Rietveld refinements of XRD patterns are listed in Table 1. The unit cell volume of $(Zn_{1/3}Nb_{1/3}Ta_{1/3})_{0.5}(Ti_{0.8}Sn_{0.2(1-y)}Ge_{0.2y})_{0.5}O_2$ was decreased with increasing of Ge^{4+} content, due to the larger ionic radius of Sn^{4+} (0.69 Å) than that of Ge^{4+} (0.53 Å) [3]. Although the ionic radius of Nb^{5+} and Ta^{5+} was same, the unit cell volume of $(Zn_{1/3}Nb_{(2-x)/3}Ta_{x/3})_{0.5}(Ti_{0.8}Sn_{0.1}Ge_{0.1})_{0.5}O_2$ was also decreased with Ta^{5+} content. These results could be explained that the lattice parameters were also affected by ionic radius as well as bond strengths of composing ions. The individual bond lengths (apical bond, d_{apical} and equatorial bond, $d_{equatorial}$) of oxygen octahedron were obtained from the lattice parameters and oxygen position parameters of tetragonal rutile structure by Rietveld refinement method [4]. The changes of crystallographic data (lattice parameter, bond length, bond length ratio) of the sintered specimens with the substitution of Ta^{5+} for Nb^{5+} and/or Ge^{4+} for Sn^{4+} should differently affect to the microwave dielectric properties because the microwave dielectric properties of rutile structure compounds were dependent on dielectric properties of composed ions as well as structural characteristics.

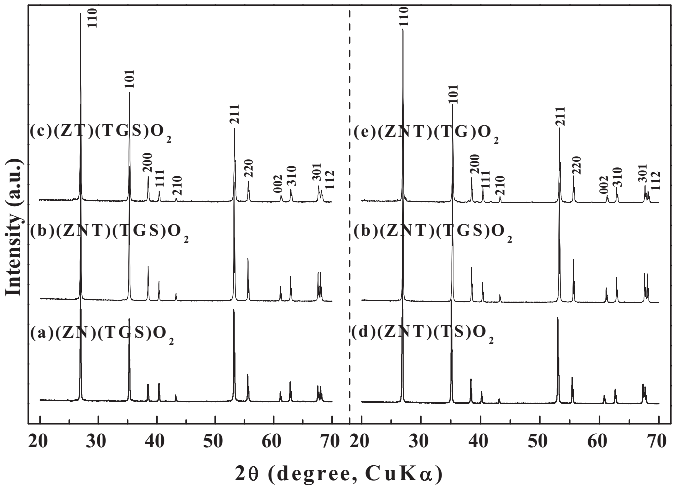

Fig. 1. X-ray diffraction of $(Zn_{1/3}Nb_{(2-x)/3}Ta_{x/3})_{0.5}(Ti_{0.8}Sn_{0.2(1-y)}Ge_{0.2y})_{0.5}O_2$ ($x = 0, 1, 2, y = 0, 0.5, 1$) sintered at 1250 °C for 3 h; (a) $(Zn_{1/3}Nb_{2/3})_{0.5}(Ti_{0.8}Sn_{0.1}Ge_{0.1})_{0.5}O_2$, (b) $(Zn_{1/3}Nb_{1/3}Ta_{1/3})_{0.5}(Ti_{0.8}Sn_{0.1}Ge_{0.1})_{0.5}O_2$, (c) $(Zn_{1/3}Ta_{2/3})_{0.5}(Ti_{0.8}Sn_{0.1}Ge_{0.1})_{0.5}O_2$, (d) $(Zn_{1/3}Nb_{1/3}Ta_{1/3})_{0.5}(Ti_{0.8}Sn_{0.2})_{0.5}O_2$, (e) $(Zn_{1/3}Nb_{1/3}Ta_{1/3})_{0.5}(Ti_{0.8}Ge_{0.2})_{0.5}O_2$.

At microwave frequencies, the dielectric constant (K) is dependent on the theoretical dielectric polarizabilities ($\alpha_{theo.}$) obtained from the additive rule [8]. Since the $\alpha_{theo.}$ of GeO_2 (5.65 Å^3) is smaller than that of SnO_2 (6.85 Å^3) [8], the K of the specimens with the substitution of Ge^{4+} for Sn^{4+} was decreased with GeO_2 content. However, the K of the specimens with the substitution of Ta^{5+} for Nb^{5+} was decreased with $(Zn_{1/3}Ta_{2/3})O_2$ content, even though the $\alpha_{theo.}$ of $(Zn_{1/3}Ta_{2/3})O_2$ (7.85 Å^3) is larger than that of $(Zn_{1/3}Nb_{2/3})O_2$ (7.35 Å^3) [8]. These results could be explained by the crystal structural characteristics of $(Zn_{1/3}Nb_{2/3})_{0.5}(Ti_{0.8}Sn_{0.1}Ge_{0.1})_{0.5}O_2$ ($(ZN)(TSG)O_2$) substituted Ta^{5+} for Nb^{5+} and/or $(Zn_{1/3}Nb_{1/3}Ta_{1/3})_{0.5}$ $(Ti_{0.8}Sn_{0.2})_{0.5}O_2$ ($(ZNT)(TS)O_2$) substituted Ge^{4+} for Sn^{4+}.

To investigate the effects of crystal structural characteristics on the K, the bond length ratios of $d_{apical}/d_{equatorial}$ were

Table 1
Crystal structure data and octahedral distortion of $(Zn_{1/3}Nb_{(2-x)/3}Ta_{x/3})_{0.5}(Ti_{0.8}Sn_{0.2(1-y)}Ge_{0.2y})_{0.5}O_2$ ($x = 0, 1, 2, y = 0, 0.5, 1$) sintered at 1250 °C for 3 h.

Composition			Lattice parameters (Å)		$V_{unit\ cell}$ (Å)	Bond length (Å)		Ratio of $d_{apical}/d_{equatorial}$	Distortion ($\Delta \times 10^5$)
x	y	Symbol	a	c		d_{apical}	$d_{equatorial}$		
0	0.5	$(ZN)(TSG)O_2$	4.726 (5)	3.059 (1)	68.318	2.027 (3)	1.991 (3)	1.018	7.18
1	0.5	$(ZNT)(TSG)O_2$	4.723 (2)	3.060 (4)	68.259	2.020 (5)	1.987 (1)	1.017	6.06
2	0.5	$(ZT)(TSG)O_2$	4.727 (2)	3.053 (3)	68.209	2.016 (3)	1.998 (5)	1.009	1.79
1	0	$(ZNT)(TS)O_2$	4.728 (1)	3.060 (6)	68.409	2.037 (3)	1.995 (5)	1.021	9.71
1	0.5	$(ZNT)(TSG)O_2$	4.723 (2)	3.060 (4)	68.259	2.020 (5)	1.987 (1)	1.017	6.06
1	1	$(ZNT)(TG)O_2$	4.722 (1)	3.058 (2)	68.173	2.020 (5)	1.999 (3)	1.011	2.44

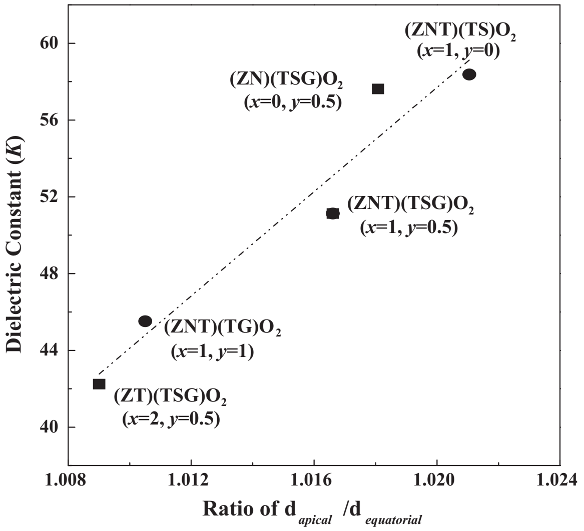

Fig. 2. Dependence of dielectric constant (K) on ratio of $d_{apical}/d_{equatorial}$ of $(Zn_{1/3}Nb_{(2-x)/3}Ta_{x/3})_{0.5}(Ti_{0.8}Sn_{0.2(1-y)}Ge_{0.2y})_{0.5}O_2$ ($x = 0, 1, 2, y = 0, 0.5, 1$) sintered at 1250 °C for 3 h.

calculated from individual bond lengths of oxygen octahedron in the unit cell of the specimens. As shown in Fig. 2, the K of the specimens was increased with the bond length ratio ($d_{apical}/d_{equatorial}$) because the larger bond length ratios of d_{apical} to $d_{equatorial}$ than unit are leading to the larger rattling space of the center ions of oxygen octahedra. Therefore, the K of rutile structure is more strongly dependent on the bond length ratio ($d_{apical}/d_{equatorial}$) than the $\alpha_{theo.}$ of the specimens.

The oxygen octahedron is expected to be distorted from the changes of bond lengths (d_{apical}, $d_{equatorial}$), and the oxygen octahedral distortion (Δ) was calculated from the individual bond length of oxygen octahedron using the Eq. (1) reported by Shannon [3].

$$\Delta = \frac{1}{6}\sum\left\{\frac{(R_i - \bar{R})}{\bar{R}}\right\}^2 \tag{1}$$

where R_i is an individual bond length, and $\bar{R}$ is average bond length of oxygen octahedron. As confirmed in Table 1, the Δ was decreased with increasing of Ta^{5+} and/or Ge^{4+} content, and the temperature coefficient of resonant frequency (TCF) also decreased with the decrease of the Δ. Dependences of TCF on the Δ of $(Zn_{1/3}Nb_{(2-x)/3}Ta_{x/3})_{0.5}(Ti_{0.8}Sn_{0.2(1-y)}Ge_{0.2y})_{0.5}O_2$ ($x = 0, 1, 2, y = 0, 0.5, 1$) are shown in Fig. 3. These results could be explained that the large positive TCF was often accompanied by the large K ($10 < K$), and the TCF was increased with increasing K for the materials with large K, because the TCF is a function of temperature coefficient of dielectric constant (TCK) ($TCF = -(1/2)TCK\text{-}\alpha$, α (thermal expansion coefficient)≒10 ppm/°C for ceramics), and TCK is a function of $(\delta\alpha_m/\delta T)_V$ (where α_m: polarizability of molar volume, T: temperature) which is always negative and decreased with increasing K in the range of $10 < K < 200$ [9]. Therefore, the changes of bond lengths (d_{apical}, $d_{equatorial}$) with the substitution of Ta^{5+} for Nb^{5+} and/or Ge^{4+} for Sn^{4+} affected to rattling space as well as Δ, and the K and TCF of the compounds with rutile structure were dependent on these changes of bond lengths.

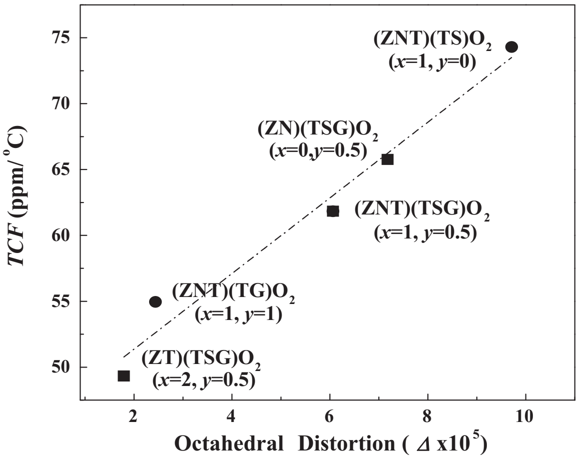

Fig. 3. Dependence of TCF on octahedral distortion of $(Zn_{1/3}Nb_{(2-x)/3}Ta_{x/3})_{0.5}(Ti_{0.8}Sn_{0.2(1-y)}Ge_{0.2y})_{0.5}O_2$ ($x = 0, 1, 2, y = 0, 0.5, 1$) sintered at 1250 °C for 3 h.

Generally, the Qf value was dependent on the extrinsic factors such as density, secondary phase, impurity and grain size, along with the intrinsic factors [10]. In these systems, the effects of the density and secondary phase could be neglected due to the higher relative density than 93%, and no secondary phase in XRD patterns. To confirm the effects of grain size on the Qf value, SEM micrographs of the specimens are shown in Fig. 4. For $(Zn_{1/3}Nb_{1/3}Ta_{1/3})_{0.5}(Ti_{0.8}Sn_{0.2(1-y)}Ge_{0.2y})_{0.5}O_2$ sintered specimens (Fig. 4(d), (b), (e)), the grain size of $(Zn_{1/3}Nb_{1/3}Ta_{1/3})_{0.5}(Ti_{0.8}Sn_{0.1}Ge_{0.1})_{0.5}O_2$ was larger than that of other specimens, which was agreed with the changes of Qf value of the specimens. However, the grain size of $(Zn_{1/3}Nb_{(2-x)/3}Ta_{x/3})_{0.5}(Ti_{0.8}Sn_{0.1}Ge_{0.1})_{0.5}O_2$ sintered specimens (Fig. 4(a), (b), (c)) was slightly decreased with Ta^{5+} content, while Qf value of the specimens was increased.

Therefore, there is an effect of the intrinsic factors on Qf values which is the minimum loss related with lattice anharmonicity that can be expected for a particular crystal structure. These can also be evaluated by the ionic packing fraction of unit cell [11]. The packing fraction defined by the summation of volume of packed ions over volume of primitive unit cell, could be obtained from Eq. (2) for AO_2 rutile compound.

$$\begin{aligned}\text{Packing fraction (\%)} &= \frac{\text{volume of pcaked ions}}{\text{volume of unit-cell}} \times Z \\ &= \frac{4\pi/3(r^3_{cations} + 2 \times r^3_{oxygen})}{a^2 \times c} \times 2\end{aligned} \tag{2}$$

where $r_{cations}$ and $r_{oxygen\ ions}$ are the effective ionic radii at each coordination number, a and c are the lattice parameters and $Z = 2$ for tetragonal rutile structure. The Qf values were improved with the increase of Ta^{5+} and/or Sn^{4+} content due to the increase of ionic packing fraction of unit-cell, and the dependence of Qf value of rutile compound on packing fraction was clearly confirmed in Fig. 5.

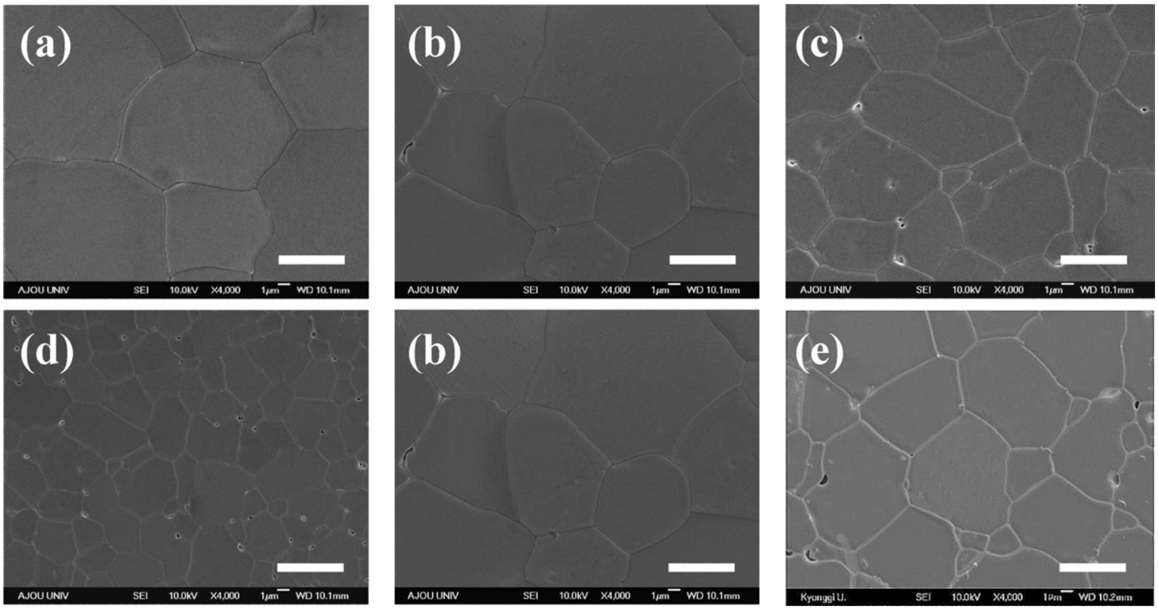

Fig. 4. SEM Photographs of $(Zn_{1/3}Nb_{(2-x)/3}Ta_{x/3})_{0.5}(Ti_{0.8}Sn_{0.2(1-y)}Ge_{0.2y})_{0.5}O_2$ ($x = 0, 1, 2$, $y = 0, 0.5, 1$) sintered at 1250 °C for 3 h; (a) $(Zn_{1/3}Nb_{2/3})_{0.5}(Ti_{0.8}Sn_{0.1}Ge_{0.1})_{0.5}O_2$, (b) $(Zn_{1/3}Nb_{1/3}Ta_{1/3})_{0.5}(Ti_{0.8}Sn_{0.1}Ge_{0.1})_{0.5}O_2$, (c) $(Zn_{1/3}Ta_{2/3})_{0.5}(Ti_{0.8}Sn_{0.1}Ge_{0.1})_{0.5}O_2$, (d) $(Zn_{1/3}Nb_{1/3}Ta_{1/3})_{0.5}(Ti_{0.8}Sn_{0.2})_{0.5}O_2$, (e) $(Zn_{1/3}Nb_{1/3}Ta_{1/3})_{0.5}(Ti_{0.8}Ge_{0.2})_{0.5}O_2$ (Bar = 5 μm).

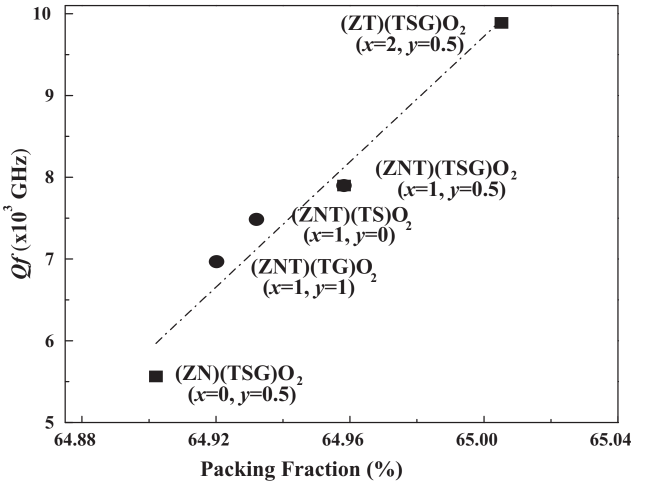

Fig. 5. Dependence of Qf value on packing fraction of $(Zn_{1/3}Nb_{(2-x)/3}Ta_{x/3})_{0.5}(Ti_{0.8}Sn_{0.2(1-y)}Ge_{0.2y})_{0.5}O_2$ ($x = 0, 1, 2$, $y = 0, 0.5, 1$) sintered at 1250 °C for 3 h.

4. Conclusion

Dependence of microwave dielectric properties on the structural characteristics of $(Zn_{1/3}Nb_{(2-x)/3}Ta_{x/3})_{0.5}(Ti_{0.8}Sn_{0.1}Ge_{0.1})_{0.5}O_2$ ($x = 0, 1, 2$) substituted Ta^{5+} for Nb^{5+} and $(Zn_{1/3}Nb_{1/3}Ta_{1/3})_{0.5}(Ti_{0.8}Sn_{0.2(1-y)}Ge_{0.2y})_{0.5}O_2$ ($y = 0, 0.5, 1$) substituted Ge^{4+} for Sn^{4+} was investigated. Single phase of tetragonal rutile structure was detected through the entire range of compositions. Dielectric constant (K) of the specimens was increased with SnO_2 and/or Nb_2O_5 content due to the increase of bond length ratio of $d_{apical}/d_{equatorial}$ of the oxygen octahedron. Temperature coefficient of resonant frequency (TCF) of the specimens could be controlled by the distortion of oxygen octahedron. Qf value was improved with Ta_2O_5 and/or SnO_2 content due to the increase of ionic packing fraction in the unit cell of crystal structure.

Acknowledgment

This work was supported by Kyonggi University Research Grant 2009.

References

[1] S.D. Mo, W.Y. Ching, Electronic and optical properties of three phases of titanium dioxide: rutile, anatase, and brookite, Physical Review B51 (1995) 13023–13032.

[2] I.M. Reany, E.L. Colla, N. Setter, Dielectric and structural characteristics of Ba- and Sr-based complex perovskites as a function of tolerance Factor, Japanese Journal of Applied Physics 33 (1994) 3984–3990.

[3] R.D. Shannon, Revised effective ionic radii and systematic studies of interatomic distances in halides and chalcogenides, Acta Crystallographica A32 (1976) 751–767.

[4] T. Roisnel, J.R. Carvajal, WinPLOTR: a Windows tool for powder diffraction pattern analysis, Materials Science Forum 378–381 (2001) 118–123.

[5] I. Abrahams, P.G. Bruce, W.I.F. David, A.R. West, Structure determination of substituted rutiles by time-of-flight neutron diffraction, Chemistry of Materials 1 (1989) 237–240.

[6] B.W. Hakki, P.D. Coleman, A dielectric resonator method of measuring inductive capacities in the millimeter range, IRE Transaction on Microwave Theory and Techniques 8 (1960) 402–410.

[7] T. Nishikawa, K. Wakino, H. Tamura, H. Tanaka, Y. Ishikawa, Precise measurement method for temperature coefficient of microwave dielectric resonator material, IEEE MTT-S International Microwave Symposium Digest 87 (1987) 277–280.

[8] R.D. Shannon, Dielectric polarizabilities of ions in oxides and fluorides, Journal of Applied Physics 73 (1993) 348–366.

[9] A.J. Bosman, E.E. Havinga, Temperature dependence of dielectric constants of cubic ionic compounds, Physical Review 129 (1963) 1593–1600.

[10] D.M. Iddles, A.J. Bell, A.J. Moulson, Relationships between dopants, microstructure and the microwave dielectric properties of ZrO_2–TiO_2–SnO_2 ceramics, Journal of Materials Science 27 (1992) 6303–6310.

[11] E.S. Kim, B.S. Chun, R. Freer, R.J. Cernik, Effects of packing fraction and bond valence on microwave dielectric properties of $A^{2+}B^{6+}O_4$ (A^{2+}: Ca, Pb, Ba; B^{6+}: Mo, W) ceramics, Journal of European Ceramic Society 30 (2010) 1731–1736.